

# Ruprecht 106: the first single population Globular Cluster?

S. Villanova and D. Geisler

*Departamento de Astronomía, Casilla 160, Universidad de Concepción, Chile*  
svillanova@astro-udec.cl

G. Carraro

*European Southern Observatory, Alonso de Cordova 3107 Vitacura, Santiago de Chile, Chile*

C. Moni Bidin

*Instituto de Astronomía, Universidad Católica del Norte, Av. Angamos 0610, Antofagasta, Chile*  
and

C. Muñoz

*Departamento de Astronomía, Casilla 160, Universidad de Concepción, Chile*

## ABSTRACT

All old Galactic Globular Clusters studied in detail to date host at least two generations of stars, where the second is formed from gas polluted by processed material produced by massive stars of the first. This process can happen if the initial mass of the cluster exceeds a threshold above which ejecta are retained and a second generation is formed. A determination of this mass-threshold is mandatory in order to understand how GCs form. We analyzed 9 RGB stars belonging to the cluster Ruprecht 106. Targets were observed with the UVES@VLT2 spectrograph. Spectra cover a wide range and allowed us to measure abundances for light (O,Na,Mg,Al),  $\alpha$  (Si,Ca,Ti), iron-peak (Sc,V,Cr,Mn,Fe,Co,Ni,Cu,Zn) and neutron-capture (Y,Zr,Ba,La,Ce,Pr,Nd,Sm,Eu,Dy,Pb) elements. Based on these abundances we show that Ruprecht 106 is the first convincing example of a single population GC (i.e. a true simple stellar population), although the sample is relatively small. This result is supported also by an independent photometric test and by the HB morphology and the dynamical state. It is old ( $\sim 12$  Gyrs) and, at odds with other GCs, has no  $\alpha$ -enhancement. The material it formed from was contaminated by both s- and r- process elements. The abundance pattern points toward an extragalactic origin. Its present day mass ( $M=10^{4.83} M_{\odot}$ ) can be assumed as a strong lower limit for the initial mass threshold below which no second generation is formed. Clearly, its initial mass must have been significantly greater but we have no current constraints on the amount of mass loss during its evolution.

*Subject headings:* globular clusters: general — globular clusters: individual(Ruprecht 106)

## 1. Introduction

Recently Globular Clusters (GCs) in the Galaxy were discovered to have chemical inhomogeneities. More specifically, Carretta et al. (2009) showed

that all GCs studied up to now have at least a spread (or anticorrelation) in the content of their light-elements O and Na. Indeed, they present a new definition of a GC as a cluster which exhibits such an anticorrelation, with the implication that

all globulars, at least those above a certain mass limit, must possess this characteristic. Many other light-elements such as C,N,Mg, and Al also show a spread or a (anti)correlation. The Na-O anticorrelation was found over the entire mass range observed, from NGC 6838 ( $M=10^{4.30} M_{\odot}$ ) up to 47 Tuc ( $M=10^{6.03} M_{\odot}$ ). This spread is probably due to the early evolution of each cluster, when a second generation of stars was born from gas polluted by ejecta of evolved stars of the first generation (the so called multiple-population phenomenon, Kraft 1994; Gratton et al. 2004, 2012; Piotto 2009; Piotto et al. 2012). According to this model, stars of the first (older) generation were born with normal He ( $Y\sim 0.25$ ) and a Na/O content similar to the field stars in the Halo, while stars of the second (younger) generation, because of this self-enrichment, are He/Na richer ( $Y\geq 0.25$ , D’Antona & Caloi 2008) and O-poorer with respect to the first generation. Several kinds of polluters have been proposed, including intermediate mass AGB stars ( $M\approx 4-8 M_{\odot}$ , Ventura et al. 2001), fast rotating massive stars ( $M>20 M_{\odot}$ , Decressin et al. 2007) massive binaries stars ( $M\approx 20 M_{\odot}$ , de Mink et al. 2009) and novae (Maccarone & Zurek 2012). In some cases also SNeII may have been at work (Marino et al. 2009). The first requirement for this process is that the initial mass of the cluster was high enough to retain both some primordial gas and the ejecta. The higher the initial mass, the higher the mass of the gas and ejecta that can be retained, and the more extended the abundance spread that is expected to be observed nowadays (D’Ercole et al. 2008). Subsequently, all clusters are expected to lose mass due to both internal and external processes.

The nature of the most effective polluter changes with cluster mass, because more massive GCs can retain faster ejecta, including those from a SNe explosion (Valcarce & Catelan 2008). This is the case for M22 (Marino et al. 2009),  $\omega$  Centauri (Johnson & Pilachowski 2010), and M54 (Carretta et al. 2010), where spread in the  $\alpha$ -element and iron content were found besides the usual light-element spread, indicating pollution by SNeII.

Lower mass GCs can retain only slow winds, such as those from massive main sequence stars or intermediate mass AGB stars where only light-

element variation is expected (as in the case of the standard globular cluster M4, Marino et al. 2008).

Below a certain mass threshold no ejecta are retained at all, so single population GCs are expected (Caloi & D’Antona 2011). Indeed, searches for light element spreads in much lower mass open clusters have been negative (de Silva et al. 2009), with the exception of NGC 6791 (Geisler et al. 2012) that, however, may not be a genuine member of this category (Carraro et al. 2012).

Carretta et al. (2009) showed that most of the stars currently found in a GC belong to the second generation ( $\sim 60\div 80\%$ ). This is at odds with theory, which says that first generation stars must have been much more numerous than we observe nowadays in order to produce enough ejecta to form the second. This contradiction can be partially explained if we assume that ejecta were collected preferentially in the center of the cluster due to the gravitational potential. Because of this the second generation was formed in the center and was much less affected by Galactic tidal disruption than the first, which lost most of its members (Caloi & D’Antona 2011).

This scenario holds also for old and intermediate-age massive clusters in the Large Magellanic Cloud (LMC, Mucciarelli et al. 2008, 2009). The former are generally more massive than the latter and appear to mimic Galactic GCs in having an extended Na/O anticorrelation, while the latter only show some spread in Na, with the possible exception of a single object (see section 5) that is doubtful. For this reason Mucciarelli et al. (2009) reiterated that mass can be the key factor in determining chemical inhomogeneities.

Recently Caloi & D’Antona (2011) suggested the possibility of the existence of two types of single population GCs. The first is represented by clusters initially not massive enough to be able to retain primordial gas and ejecta from evolved stars and form a second generation of stars. The second is represented by massive clusters that retained almost all the first generation and so only a small fraction of the stars would belong to the second generation population. Such clusters would preferentially be those that do not fill their tidal radius. These second are only pseudo-single population clusters, because the second generation of

stars is just very small compared to the first generation, but still present. Caloi & D’Antona (2011) presented Palomar 3 as a probable example of the first type because of the small color spread of its horizontal branch (HB), of only  $\sim 0.25$  mag in B-V (see their Fig. 2).

A key question is if there is any relatively massive globular cluster that is composed of only chemically homogeneous stars. Such a cluster should be sought among the less massive globulars in the Galaxy. For this reason we focused our investigation on Ruprecht 106 ( $M \sim 10^{4.8} M_{\odot}$ , Mandushev et al. 1991). This cluster was first studied by Buonanno et al. (1990) who suggested an age 4-5 Gyrs younger than the oldest halo GCs and a metallicity of  $[Fe/H] \sim -2.0$  based on photometric indicators. Francois et al. (1997) gave  $[Fe/H] \sim -1.6$ , based on spectroscopic observations. According to the most recent work by Dotter et al. (2011) Ruprecht 106 is a relatively old, metal-poor (11.5 Gyrs,  $[Fe/H] \sim -1.5$ ) GC with a solar scaled  $\alpha$ -element content.

We selected this cluster, apart from its low mass, for the small extension of its HB. According to D’Antona et al. (2002), the extension of the HB in a GC is proportional to the amount of helium variation due to self-pollution among its stars. He-normal stars are located in the redder part of the HB, while He-rich stars lie in the bluer part, as recently shown by Marino et al. (2011) and Gratton et al. (2011, 2012, 2013).

Caloi & D’Antona (2011) suggest that the best candidates for single population GCs are those with both stubby HBs for their metallicity and with  $M < 10^{4.8} M_{\odot}$ . Ruprecht 106 fulfills both of these characteristics but was not investigated by them.

So an HB with a small extension may indicate no spread in helium (or light-elements) and the absence of the self-pollution phenomenon. In such a cluster only one generation (the first) should be present. It should also have a homogeneous content of all the other elements ( $\alpha$ , iron-peak, s and r). The scenario is complicated by the fact that age and mass-loss are also involved. In fact a young cluster (less than 10 Gyrs) could show no color spread on the HB (that would appear entirely red) but still have a variation in He just because HB stars do not have a low enough mass to be located in the blue part (the younger the

age, the higher the mean mass in the HB). On the other hand a differential mass-loss along the HB can generate a spread on the HB even if no He variation is present. Ruprecht 106 is old and metal poor, so it should have a blue HB, or at least some of the HB stars should be located on the blue HB, as in M4 or NGC 6752, two clusters with an extended and well studied Na-O anticorrelation (Marino et al. 2008; Carretta et al. 2007b). In spite of this, Dotter et al. (2011) show a CMD (see Fig. 1) with only a red and slightly extended HB. The color baseline of the HB is  $\sim 0.2$  mag, less than Palomar 3, which was proposed by Caloi & D’Antona (2011) as a probable single population cluster. For all these reasons we selected it as a good candidate single population GC. In order to prove if this is true, we analyzed spectra for a statistically significant sample of RGB stars and measured their chemical composition. If it indeed is a single population cluster we should observe a homogeneous content of all the elements, within the observational errors.

In section 2 we describe data reduction and in section 3 the methodology we used to obtain the chemical abundances. In section 4 we present our results including a comparison with the literature. In section 5 and 6 we discuss Ruprecht 106 as a single population GC, and in section 7 we compare it with different formation environments (Galactic and extragalactic). Finally in section 8 we give a summary of our findings.

## 2. Observations and data reduction

Our dataset consists of high resolution spectra collected in 2002 and downloaded from the Advanced Data Products ESO archive <sup>1</sup>. The spectra were obtained with the UVES spectrograph, mounted at the VLT telescope. A total of 10 stars were observed between  $V=14.4$  and  $V=16.5$ , from the RGB-bump up to the RGB-tip of the cluster (see Fig. 1). All stars were observed with the blue and red arms of the spectrograph, and spectra cover a range of 3700–6800 Å. The signal-to-noise (S/N) is between 50 and 70 at 6000 Å.

Data were reduced using the dedicated pipeline (see <http://www.eso.org/sci/software/pipelines/>). Data reduction includes bias subtraction, flat-field

<sup>1</sup>[http://archive.eso.org/eso/eso\\_archive\\_adp.html](http://archive.eso.org/eso/eso_archive_adp.html)

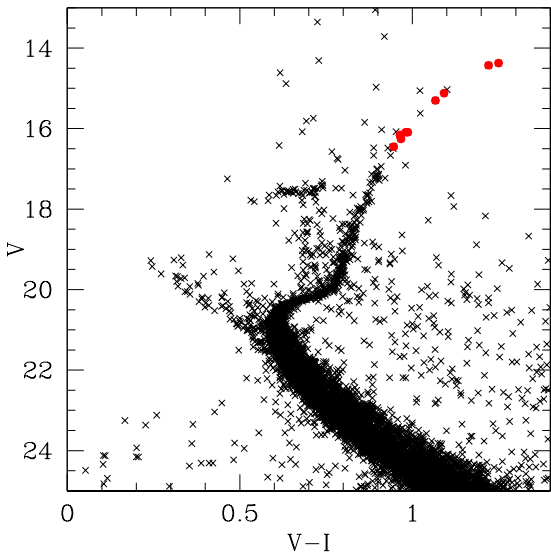


Fig. 1.— The CMD of Ruprecht 106 with the observed RGB stars indicated as filled red circles (Dotter et al. 2011).

correction, wavelength calibration, sky subtraction, and spectral rectification.

Radial velocities were measured by the *fxcor* package in IRAF, using a synthetic spectrum as a template. One star turned out to have a very different radial velocity, and so was rejected as a non-member. The mean heliocentric value for our member targets is  $-38.4 \pm 0.4$  km/s. Da Costa et al. (1992) gives  $-44 \pm 3$  km/s. There is a discrepancy between the two results; however, it is not dramatic and due probably to the low resolution of Da Costa et al. (1992) spectra ( $\Delta\lambda=3.2$  Å).

Table 1 lists the basic parameters of the member stars: ID (from Buonanno et al. 1990), J2000.0 coordinates (RA & DEC), ACS@HST V and I magnitudes (Sarajedini, private communication), heliocentric radial velocity ( $RV_H$ ),  $T_{\text{eff}}$ ,  $\log(g)$ , micro-turbulence velocity ( $v_t$ ), and metallicity ( $[\text{Fe}/\text{H}]$ ). The determination of the atmospheric parameters is discussed in the next section.

### 3. Abundance analysis

The chemical abundances for Mg, Si, Ca, Ti, Cr, Fe, and Ni were obtained using the equivalent

widths (EQWs) method. See Marino et al. (2008) for a more detailed explanation of the method we used to measure the EQWs. For the other elements (O, Na, Al, Sc, V, Mn, Co, Cu, Zn, Y, Zr, Ba, La, Ce, Pr, Nd, Sm, Eu, Dy, Pb), whose lines are affected by blending, we used the spectrum-synthesis method. For this purpose we calculated 5 synthetic spectra having different abundances, and estimated the best-fitting value as the one that minimizes the r.m.s. scatter. Si presents few features in the spectrum, so in this case abundances derived from the EQWs were cross-checked with the spectral synthesis method in order to obtain more accurate measurements. Only lines not contaminated by telluric features were used.

Initial atmospheric parameters were obtained in the following way. First,  $T_{\text{eff}}$  was derived from the V-I color using the relation of Alonso et al. (1999) and the reddening ( $E(B-V)=0.20$ ) from Harris (1996). Surface gravities ( $\log(g)$ ) were obtained from the canonical equation:

$$\log\left(\frac{g}{g_{\odot}}\right) = \log\left(\frac{M}{M_{\odot}}\right) + 4 \log\left(\frac{T_{\text{eff}}}{T_{\odot}}\right) - \log\left(\frac{L}{L_{\odot}}\right).$$

where the mass  $M/M_{\odot}$  was assumed to be  $0.8 M_{\odot}$ , and the luminosity  $L/L_{\odot}$  was obtained from the absolute magnitude  $M_V$  assuming an apparent distance modulus of  $(m-M)_V=17.25$  (Harris 1996). The bolometric correction (BC) was derived by adopting the relation BC- $T_{\text{eff}}$  from Alonso et al. (1999). Finally, micro-turbulence velocity ( $v_t$ ) was obtained from the relation of Marino et al. (2008).

These atmospheric parameters were considered as initial estimates and were refined during the abundance analysis. As a first step, atmospheric models were calculated using ATLAS9 (Kurucz 1970) assuming the initial estimate of  $T_{\text{eff}}$ ,  $\log(g)$ , and  $v_t$ , and the  $[\text{Fe}/\text{H}]$  value from Harris (1996) ( $[\text{Fe}/\text{H}]=-1.68$ ).

Then  $T_{\text{eff}}$ ,  $v_t$ , and  $\log(g)$  were adjusted and new atmospheric models calculated in an interactive way in order to remove trends in Excitation Potential (E.P.) and equivalent width vs. abundance for  $T_{\text{eff}}$  and  $v_t$  respectively, and to satisfy the ionization equilibrium for  $\log(g)$ . FeI and FeII were used for this latter purpose. The  $[\text{Fe}/\text{H}]$  value of the model was changed at each iteration according to the output of the abundance

TABLE 1  
BASIC PARAMETERS OF THE OBSERVED STARS.

ID	RA(h:m:s)	DEC(°:':")	V(mag)	I(mag)	RV <sub>H</sub> (km/s)	T <sub>eff</sub> (K)	log(g)(dex)	v <sub>t</sub> (km/s)	[Fe/H]
Ru <sub>1445</sub>	12:38:39.2	-51:08:41.4	16.257	15.290	-40.26	4580	0.80	1.52	-1.52
Ru <sub>1614</sub>	12:38:36.4	-51:08:24.5	14.373	13.123	-36.53	4020	0.00	1.80	-1.44
Ru <sub>1863</sub>	12:38:34.9	-51:08:03.8	16.090	15.109	-37.79	4600	1.00	1.50	-1.49
Ru <sub>1951</sub>	12:38:35.2	-51:07:51.6	15.120	14.028	-36.51	4380	0.60	1.60	-1.39
Ru <sub>2004</sub>	12:38:40.7	-51:07:46.1	14.427	13.206	-39.12	4140	0.10	1.74	-1.46
Ru <sub>2032</sub>	12:38:48.8	-51:07:43.2	16.160	15.196	-38.25	4570	1.05	1.44	-1.49
Ru <sub>676</sub>	12:38:44.0	-51:09:51.7	16.091	15.104	-38.51	4550	0.85	1.50	-1.52
Ru <sub>801</sub>	12:38:36.2	-51:09:37.6	16.450	15.504	-39.56	4600	0.95	1.51	-1.51
Ru <sub>970</sub>	12:38:42.4	-51:09:22.3	15.301	14.234	-39.41	4400	0.55	1.60	-1.42

analysis. The Local Thermodynamic Equilibrium (LTE) program MOOG (Snedden 1973) was used for the abundance analysis. Na is known to be affected by departure from LTE, so we applied the Mashonkina et al. (2000) NLTE correction to our Na abundances. Due to the small T<sub>eff</sub> range covered by our stars, we decided to apply a mean correction of -0.20 dex to all the stars.

The linelist is that used in previous papers (e.g. Villanova & Geisler 2011), so we refer to those articles for detailed discussion about this point. The adopted solar abundances we used are reported in Tab. 2 and agree well with those given by Grevesse & Sauval (1998).

Apart from elements already measured in our previous papers, here we added Sc (5684 Å line), V (6275 and 6285 Å lines), Mn (5420 Å line), Co (5248 Å line), Cu (5218 Å line), Zn (4811 Å line), La (5123 Å line), Ce (5274 Å line), Pr (4497 Å line), Nd (5320 Å line), Sm (4499 Å line), Dy (5170 Å line), Pb (4058 Å line). We could measure Al only for the star Ru<sub>1614</sub>. For the other targets we give upper limits. Element abundances are reported in Tab. 2 and Fig. 2.

A detailed internal error analysis was performed by varying T<sub>eff</sub>, log(g), [Fe/H], and v<sub>t</sub> and redetermining abundances of star #Ru<sub>1951</sub>, assumed to represent the entire sample. Parameters were varied by ΔT<sub>eff</sub>=+30 K, Δlog(g)=+0.09, Δ[Fe/H]=+0.05 dex, and Δv<sub>t</sub>=+0.03 km/s. This estimation of the internal errors for atmospheric parameters was performed as in Marino et al. (2008). Results are shown in Tab. 3, including

the error due to the noise of the spectra. This error was obtained for elements whose abundance was obtained by EQWs, as the average value of the errors of the mean given by MOOG, and for elements whose abundance was obtained by spectrum-synthesis, as the error given by the fitting procedure. σ<sub>tot</sub> is the squared sum of the single errors, while σ<sub>obs</sub> is the mean observed dispersion. The agreement between the two values is well within 3σ for all elements, indicating that there is no evidence for chemical inhomogeneity for the 9 giants studied in Ruprecht 106. This is our principle finding. Only for Ce we have a 3σ difference, while for Sm σ<sub>tot</sub> differs from σ<sub>obs</sub> by 6σ and is larger. This suggests some overestimation of the internal error.

#### 4. Results and comparison with literature

In the following sections, we will discuss in detail our results. In addition, we will compare them with the literature, and specifically with Buonanno et al. (1990), Sarajedini & Layden (1997), Da Costa et al. (1992), Francois et al. (1997), Brown et al. (1997), Dotter et al. (2011). The first two give a photometric metallicity, while the third and the fourth give a spectroscopic metallicity using low-resolution spectra. Da Costa et al. (1992) use the Ca triplet method, while Francois et al. (1997) use a global-fitting of the 4780÷5300 Å region including all the spectral lines. The fifth gives a metallicity based on high-resolution spectra including [Fe/H] and [O/Fe]. Buonanno et al. (1990) and Dotter et al. (2011)

TABLE 2

COLUMNS 2-10: ABUNDANCES OF THE OBSERVED STARS. COLUMN 11: MEAN ABUNDANCE FOR THE CLUSTER. COLUMN 12: ABUNDANCES ADOPTED FOR THE SUN IN THIS PAPER. ABUNDANCES FOR THE SUN ARE INDICATED AS  $\text{LOG}\epsilon(\text{EL.})$

El.	Ru <sub>1445</sub>	Ru <sub>1614</sub>	Ru <sub>1863</sub>	Ru <sub>1951</sub>	Ru <sub>2004</sub>	Ru <sub>2032</sub>	Ru <sub>676</sub>	Ru <sub>801</sub>	Ru <sub>970</sub>	Cluster	Sun
[O/Fe]	-0.15	+0.02	-0.13	-0.06	-0.03	+0.00	-0.10	-0.05	-0.14	-0.07±0.02	8.83
[Na/Fe]	-0.41	-0.45	-0.44	-0.56	-0.50	-0.46	-0.43	-0.51	-0.44	-0.46±0.02	-
[Na/Fe] <sub>NLTE</sub>	-0.61	-0.65	-0.64	-0.76	-0.70	-0.66	-0.63	-0.71	-0.64	-0.66±0.02	6.32
[Mg/Fe]	-0.07	-0.03	-0.04	+0.03	-0.05	-0.02	+0.00	+0.04	-0.03	-0.02±0.01	7.56
[Al/Fe]	<-0.31	-0.43	<-0.54	<-0.24	<-0.47	<-0.54	<-0.01	<+0.08	<-0.41	-0.43±0.10	6.43
[Si/Fe]	+0.09	+0.03	-0.02	-0.02	-0.06	+0.03	-0.03	+0.04	-0.08	+0.00±0.02	7.61
[Ca/Fe]	+0.06	-0.10	+0.02	+0.00	-0.03	+0.00	+0.03	-0.01	+0.04	+0.00±0.02	6.39
[Sc/Fe]	-0.45	-0.29	-0.41	-0.33	-0.28	-0.34	-0.40	-0.36	-0.47	-0.37±0.03	3.12
[Ti/Fe]	-0.07	-0.06	-0.07	-0.02	-0.02	-0.05	-0.08	-0.16	-0.03	-0.06±0.01	4.94
[V/Fe]	-0.44	-0.60	-0.54	-0.58	-0.51	-	-	-	-0.53	-0.53±0.02	4.00
[Cr/Fe]	-0.16	-0.14	-0.18	-0.08	-0.11	-0.17	-0.14	-0.17	-0.12	-0.14±0.01	5.63
[Mn/Fe]	-0.34	-0.38	-0.33	-0.33	-0.28	-0.38	-0.40	-0.42	-0.30	-0.35±0.02	5.37
[Fe/H]	-1.52	-1.44	-1.49	-1.39	-1.46	-1.49	-1.52	-1.51	-1.42	-1.47±0.02	7.50
[Co/Fe]	-0.15	-0.08	-0.11	-0.30	-0.12	-	-0.05	-	-	-0.14±0.04	4.93
[Ni/Fe]	-0.29	-0.25	-0.26	-0.28	-0.24	-0.34	-0.31	-0.37	-0.27	-0.29±0.01	6.26
[Cu/Fe]	-0.71	-0.88	-0.76	-0.86	-0.80	-	-	-0.72	-0.74	-0.78±0.03	4.19
[Zn/Fe]	-0.04	-0.02	-0.30	-0.13	-0.20	-0.30	-0.30	-0.31	-0.22	-0.20±0.04	4.61
[Y/Fe]	-0.79	-0.67	-0.74	-0.65	-0.63	-0.75	-0.80	-0.80	-0.69	-0.72±0.02	2.25
[Zr/Fe]	-0.18	-0.27	-0.15	-0.26	-0.22	-0.16	-0.12	-0.09	-0.09	-0.19±0.02	2.56
[Ba/Fe]	-0.53	-0.42	-0.46	-0.46	-0.41	-0.42	-0.55	-0.45	-0.47	-0.46±0.02	2.34
[La/Fe]	-0.33	-0.25	-0.26	-0.26	-0.25	-0.23	-0.31	-0.27	-0.31	-0.27±0.01	1.26
[Ce/Fe]	-0.54	-0.60	-0.54	-0.59	-0.64	-0.59	-0.56	-0.50	-0.65	-0.58±0.02	1.53
[Pr/Fe]	-	-0.15	-0.18	-0.23	-0.13	-	-	-	-	-0.17±0.02	0.71
[Nd/Fe]	-0.42	-0.39	-0.40	-0.38	-0.43	-0.43	-0.42	-0.35	-0.37	-0.40±0.01	1.59
[Sm/Fe]	-	-0.11	-	-0.08	-0.04	-0.02	-	-	-0.12	-0.07±0.02	0.96
[Eu/Fe]	-0.23	-0.13	-0.20	-0.18	-0.07	-0.16	-0.28	-0.16	-0.26	-0.19±0.02	0.52
[Dy/Fe]	-	-0.60	-	-0.37	-0.36	-	-0.18	-0.28	-0.19	-0.33±0.06	1.10
[Pb/Fe]	-0.20	-0.21	-0.34	-0.40	-0.25	-0.27	-0.30	-0.12	-0.19	-0.25±0.03	1.98



also discuss the age of the cluster.

#### 4.1. Iron-peak and $\alpha$ elements

We found a mean  $[\text{Fe}/\text{H}]$  value for the cluster of:

$$[\text{Fe}/\text{H}]=-1.47\pm 0.02 \text{ dex}$$

All the other Fe-peak elements (Sc, V, Cr, Mn, Co, Ni, Cu, and Zn) are underabundant with respect to Fe, with a range for  $[\text{El}/\text{Fe}]$  between -0.14 dex (Cr and Co) and -0.78 dex (Cu). The chemical abundances for the  $\alpha$  elements O, Mg, Si, Ca, and Ti listed in Table 2 are solar scaled or slightly underabundant. If we use Mg, Si, Ca, and Ti to estimate a mean  $\alpha$ -element value (O will be treated separately) we obtain:

$$[\alpha/\text{Fe}]=-0.02\pm 0.01 \text{ dex}$$

We conclude that the cluster is solar-scaled as far as  $\alpha$ -elements are concerned, in agreement with Brown et al. (1997), and at odds with all the other Galactic GCs of low metallicity. However this behavior is common among extragalactic objects. We will further discuss  $\alpha$  and iron-peak elements in section 7.

Our results permit us also to explain the disagreement of metallicities in the literature. Many authors (Buonanno et al. 1990,  $[\text{Fe}/\text{H}]\sim -2$ ; Sarajedini & Layden 1997,  $[\text{Fe}/\text{H}]=-1.90$ ; Da Costa et al. 1992,  $[\text{Fe}/\text{H}]=-1.69$ ; Francois et al. 1997,  $[\text{Fe}/\text{H}]=-1.9$ ) who obtained a metallicity based on photometry (slope and/or color of the RGB) or low-resolution spectroscopy (Ca triplet or comparison with low-resolution synthetic spectra) implicitly assumed a typical halo alpha-enhancement, as in all other Galactic GCs. This fact led them to underestimate the cluster metallicity because Ruprecht 106 simply is not  $\alpha$ -enhanced, so, for a given metallicity ( $[\text{Fe}/\text{H}]$ ) the RGB-slope is larger or low resolution spectra are apparently more metal-poor (e.g. the EQW of the Ca triplet is smaller) with respect to any other GC with similar iron content. Brown et al. (1997) ( $[\text{Fe}/\text{H}]=-1.45$ ) instead obtained a more reliable result because they measured directly Fe lines. Their value is in excellent agreement with our.

#### 4.2. Neutron-capture elements

We measured neutron-capture elements from Y to Pb. They are produced through the capture of a neutron by a iron-peak seed nucleus. Once captured, the neutron decays into a proton, and a new nucleus with higher atomic number is formed. The capture can be considered slow if the timescale for the neutron capture is large compared to the timescale of the nuclear decay. In this case we have the s-process. In the case that the neutron capture is rapid compared with the timescale of the decay, we have the r-process. The distribution of neutron-capture elements is different in the two cases, and a study of their relative abundance gives information on the relative importance of the two processes on the contamination of the gas the cluster was formed from. Because the s-process happens in low-mass AGB stars (1.5-3  $M_{\odot}$ , Busso et al. 2001), intermediate mass AGB stars (4-8  $M_{\odot}$ , Karakas & Lattanzio 2007), and possibly also in massive stars ( $M > 20 M_{\odot}$ , Pignatari et al. 2008), while the r-process most probably occurs in SNeII explosions, abundances of neutron-capture elements tell us how these kind of stars contributed to the formation of the cluster. For this purpose in Fig. 3 we plotted the abundance of Ba, La, Pr, Nd, Sm, Eu, Dy, and Pb. On our data we superposed the two abundance curves of the pure s (dashed black line) and r (continuous black line) process taken from Sneden et al. (2008). Ba and Pb were used to set the zero-point of the pure s and pure r process curves (see below), while La, Pr, Nd, Sm, Eu, and Dy are those elements more sensitive to the s and r processes. The Ce abundance does not follow any curve in Fig. 3, probably because of some non-negligible systematic error in our abundance estimation for this element, so we decided not to use it in our investigation. The two curves were shifted in the y direction in order to match the Ba and Pb abundances that are the same for the two processes. Abundances of the other elements are in between the two curves and the best fitting line (the blue continuous line) indicates that r-process contributed 66% and s-process 34% to the cluster abundances. This result is confirmed by the mean  $\log\epsilon(\text{La}/\text{Eu})$  of the cluster, that is:

$$\log\epsilon(\text{La}/\text{Eu})=0.65\pm 0.02$$

According to Roederer et al. (2009, Fig. 4), this corresponds to a contribution of 71% from the r-process. We can summarize these results by estimating that r-process contributed a  $68.5 \pm 2.5\%$  and s-process a  $31.5 \pm 2.5\%$  to the contamination of the primordial gas the cluster was formed from.

## 5. Ruprecht 106 as the first single population GC

As mentioned in the Introduction, other GCs have been proposed as single population objects, like Palomar 3 (Caloi & D’Antona 2011), due to the small extension of its red HB. Kock et al. (2009) studied spectroscopically four bright RGB stars in this cluster, but due to the low S/N and the small statistics they could not prove the presence or absence of a spread in light elements, and so they could not confirm or reject the Caloi & D’Antona (2011) hypothesis. The main aim of this paper is to verify if Ruprecht 106 might be the first bonafide example of a single population old Galactic GC. For this purpose we report in Fig. 4 the Na-O abundances of our 9 stars (black points with errorbars). In this figure, for comparison, we report also data for the GCs studied in Carretta et al. (2009, filled cyan squares), NGC 1851 (Villanova et al. 2010, filled blue circles), NGC 2808 (Carretta et al. 2006, filled black squares), M4 (Villanova & Geisler 2011, open magenta circles), M22 (Marino et al. 2009, open red squares), old (filled green circles) and intermediate-age (other open green symbols) clusters in the LMC studied by Mucciarelli et al. (2008, 2009), and the Sagittarius cluster Terzan 7 (Sbordone et al. 2007, open black stars). Open red stars represent the two targets in Ruprecht 106 studied by Brown et al. (1997). These stars are #Ru<sub>1614</sub> and #Ru<sub>2004</sub> and the authors find  $[O/Fe]=-0.05, +0.08$  and  $[Na/Fe]=-0.47, -0.44$  respectively. Their Na abundance is based on the 8190 Å doublet so, according to Mashonkina et al. (2000), a NLTE correction of  $\sim -0.2$  dex looks appropriate. The agreement with our results is good.

Ruprecht 106 stars define a clump at  $[O/Fe]=-0.07$  dex and  $[Na/Fe]=-0.66$  dex that has no intrinsic dispersion. This is confirmed by Tab. 3, where the theoretical spread ( $\sigma_{tot}$ ) matches very well within the errors with the observed spread

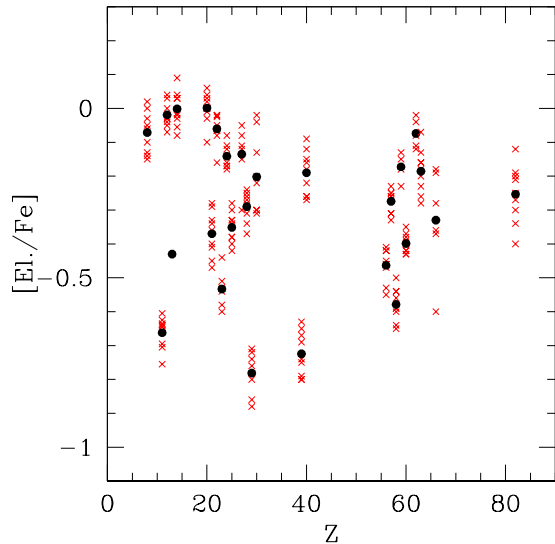


Fig. 2.— Element abundance for the single stars (red crosses) and for the cluster mean (black filled circles). See text for more details.

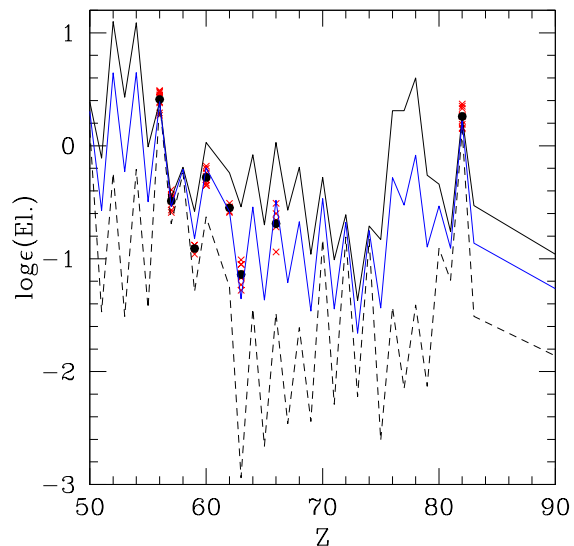


Fig. 3.— Abundance pattern of heavy neutron-capture elements. Red points represent single stars, while black points the mean abundance for the cluster. Continuous and dashed lines are pure r and s process patterns respectively. Continuous blue line is the best fit to our data.



TABLE 3  
ESTIMATED ERRORS ON ABUNDANCES DUE TO ERRORS ON ATMOSPHERIC PARAMETERS AND TO  
SPECTRAL NOISE COMPARED WITH THE OBSERVED ERRORS.

ID	$\Delta T_{\text{eff}}=30$ K	$\Delta \log(g)=0.09$	$\Delta v_t=0.03$ km/s	$\Delta [\text{Fe}/\text{H}]=0.05$	S/N	$\sigma_{\text{tot}}$	$\sigma_{\text{obs}}$
$\Delta([\text{O}/\text{Fe}])$	0.03	0.06	0.03	0.02	0.02	0.08	$0.06 \pm 0.02$
$\Delta([\text{Na}/\text{Fe}])$	0.01	0.01	0.00	0.01	0.05	0.05	$0.05 \pm 0.01$
$\Delta([\text{Mg}/\text{Fe}])$	0.02	0.01	0.00	0.01	0.05	0.06	$0.04 \pm 0.01$
$\Delta([\text{Al}/\text{Fe}])$	0.01	0.00	0.01	0.01	0.05	0.08	-
$\Delta([\text{Si}/\text{Fe}])$	0.03	0.01	0.01	0.01	0.05	0.06	$0.05 \pm 0.01$
$\Delta([\text{Ca}/\text{Fe}])$	0.00	0.00	0.00	0.00	0.04	0.04	$0.05 \pm 0.01$
$\Delta([\text{Sc}/\text{Fe}])$	0.04	0.05	0.02	0.01	0.01	0.07	$0.07 \pm 0.02$
$\Delta([\text{Ti}/\text{Fe}])$	0.02	0.00	0.00	0.01	0.03	0.04	$0.04 \pm 0.01$
$\Delta([\text{V}/\text{Fe}])$	0.02	0.01	0.00	0.01	0.08	0.08	$0.06 \pm 0.02$
$\Delta([\text{Cr}/\text{Fe}])$	0.02	0.00	0.00	0.00	0.03	0.04	$0.03 \pm 0.01$
$\Delta([\text{Mn}/\text{Fe}])$	0.01	0.01	0.01	0.00	0.04	0.04	$0.05 \pm 0.01$
$\Delta([\text{Fe}/\text{H}])$	0.04	0.01	0.01	0.01	0.01	0.05	$0.05 \pm 0.01$
$\Delta([\text{Co}/\text{Fe}])$	0.01	0.00	0.00	0.01	0.08	0.08	$0.09 \pm 0.03$
$\Delta([\text{Ni}/\text{Fe}])$	0.00	0.00	0.00	0.00	0.02	0.02	$0.04 \pm 0.01$
$\Delta([\text{Cu}/\text{Fe}])$	0.01	0.00	0.00	0.01	0.05	0.05	$0.07 \pm 0.02$
$\Delta([\text{Zn}/\text{Fe}])$	0.06	0.02	0.01	0.01	0.08	0.10	$0.11 \pm 0.03$
$\Delta([\text{Y}/\text{Fe}])$	0.04	0.04	0.02	0.00	0.08	0.10	$0.07 \pm 0.02$
$\Delta([\text{Zr}/\text{Fe}])$	0.05	0.04	0.02	0.02	0.04	0.08	$0.07 \pm 0.02$
$\Delta([\text{Ba}/\text{Fe}])$	0.02	0.05	0.02	0.03	0.01	0.07	$0.05 \pm 0.01$
$\Delta([\text{La}/\text{Fe}])$	0.04	0.03	0.02	0.00	0.02	0.06	$0.04 \pm 0.01$
$\Delta([\text{Ce}/\text{Fe}])$	0.05	0.04	0.01	0.01	0.04	0.08	$0.05 \pm 0.01$
$\Delta([\text{Pr}/\text{Fe}])$	0.02	0.04	0.01	0.00	0.05	0.07	$0.04 \pm 0.02$
$\Delta([\text{Nd}/\text{Fe}])$	0.02	0.03	0.01	0.00	0.02	0.04	$0.03 \pm 0.01$
$\Delta([\text{Sm}/\text{Fe}])$	0.02	0.05	0.03	0.02	0.07	0.10	$0.04 \pm 0.01$
$\Delta([\text{Eu}/\text{Fe}])$	0.04	0.05	0.03	0.02	0.02	0.08	$0.07 \pm 0.02$
$\Delta([\text{Dy}/\text{Fe}])$	0.01	0.07	0.02	0.01	0.02	0.08	$0.15 \pm 0.04$
$\Delta([\text{Pb}/\text{Fe}])$	0.04	0.01	0.01	0.02	0.03	0.06	$0.09 \pm 0.02$

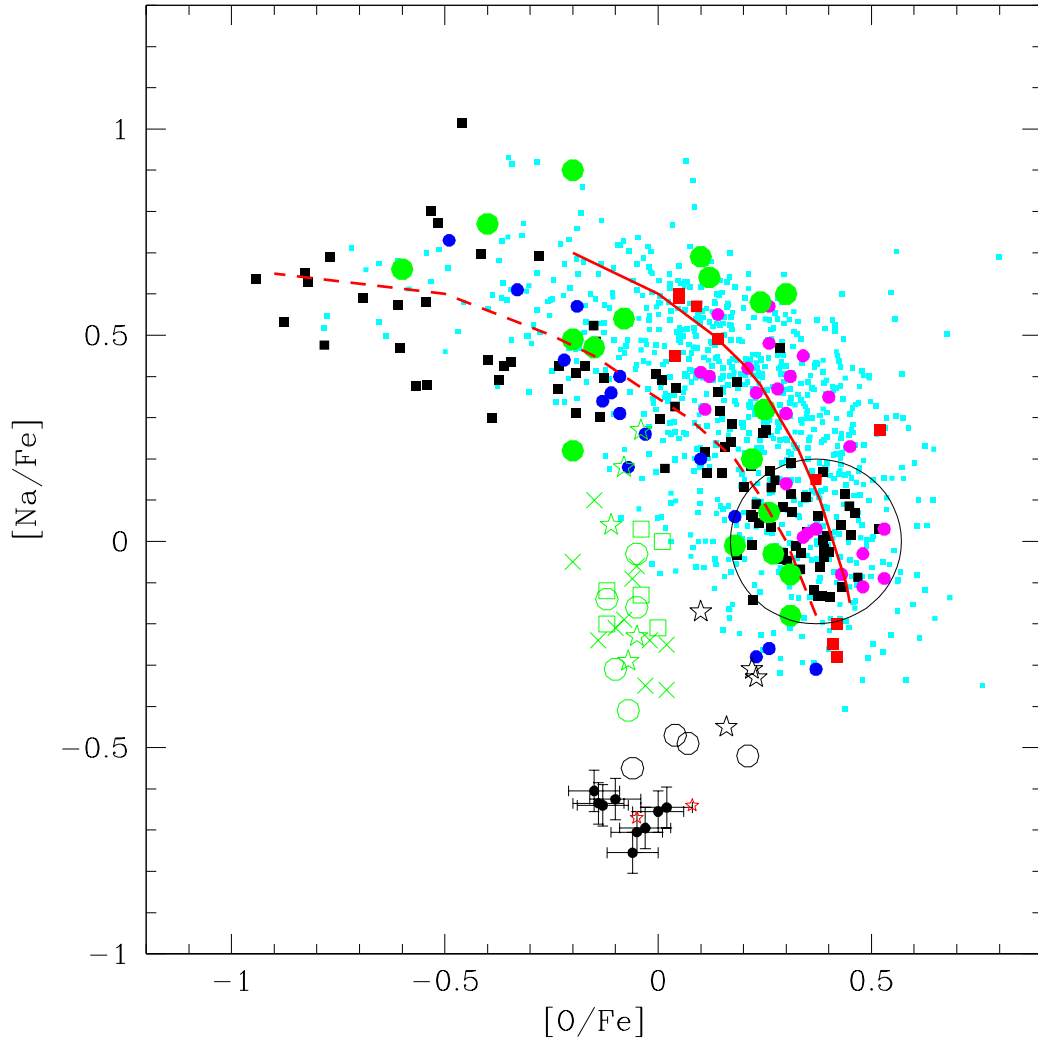


Fig. 4.—  $[\text{Na}/\text{Fe}]$  vs.  $[\text{O}/\text{Fe}]$  in GCs. Filled cyan squares: GCs from Carretta et al. (2009). Filled blue circles: NGC 1851. Filled black squares: NGC 2808. Filled red squares: M22. Filled magenta circles: M4. Filled green circles: Old LMC clusters. Open green symbols: intermediate-age LMC clusters. Open black stars: Terzan 7. Filled black circles: Ruprecht 106 (this paper). Open red stars: Ruprecht 106 by Brown et al. (1997). See text for more details.

$(\sigma_{\text{obs}})$  both for O and Na. This is true also for the other elements. This confirms our initial hypothesis that Ruprecht 106 is the first example of a single population GC, although it is possible that nature has conspired against us and we simply did not detect a true spread. See below for further discussion of this point. Recall that the

Na-O anticorrelation has been used to define a GC (Carretta et al. 2009), so its absence in Ruprecht 106 is of particular importance.

However Fig. 4 has several other interesting implications. First of all Ruprecht 106 occupies a totally unique position in this diagram (see Sec-

tion 7 for further discussion). In addition, among Galactic GCs at least two distinct Na-O anticorrelations appear, that are plotted as red lines. One is O-richer (continuous line) and represented by the trend of the stars in M4 and M22, while the other is O-poorer (dashed line) and represented by the trend of the stars in NGC 1851 and NGC2808. This fact can be explained by the  $\alpha$ -enhancement a cluster was formed with and remembering that O is an  $\alpha$  element too. If first generation stars in a cluster were born relatively O-poor (with respect to the continuous line of Fig. 4), second generation stars will also share the same chemical behavior.

As an example, NGC 1851 and M4 have a difference in their  $\alpha$ -enhancement of 0.07 dex (as defined by the mean abundance of Si and Ca), while the difference between their O content is  $\sim 0.1$  dex among the entire Na-O anticorrelation. So the O content of second generation stars does not depend only on the internal chemical evolution of the clusters, but also on the primordial O abundance of the progenitor cloud.

Old LMC clusters also follow the general Galactic trend, but this is not the case for intermediate-age LMC clusters and Terzan 7 which do not show an appreciable spread in O. On the other hand three of them show a possible spread in Na (NGC 1651: open green circles, NGC 1978: green crosses, NGC 2173: open green stars). NGC 1978 also shows a hint of a Na-O anticorrelation. Only two clusters (NGC 1783: open green squares) and Terzan 7 have a small dispersion in Na, possibly compatible with zero, but still larger than Ruprecht 106, but all of these samples are relatively small.

In Fig. 4 the region presumably inhabited by first generation stars in Galactic and LMC globular cluster is indicated by a large black circle. Even if Ruprecht 106 does not fit at all with any known Milky Way or LMC cluster, we can still state that these stars still correspond to the first generation. This is because this first generation is characterized by the fact that  $[O/Fe]=[ \alpha/Fe]$  within 0.1 dex (where  $\alpha$  is defined as the mean abundance of Si and Ca). Second generations stars have  $[O/Fe]<[ \alpha/Fe]$ . As an example, in M4 stars of the first generation ( $[ \alpha/Fe]=+0.42$ ) have  $[O/Fe]=+0.42$  dex, while stars of the second have  $[O/Fe]=+0.25$  (the difference with respect to the  $\alpha$ -enhancement is -0.17 dex). This behavior

is expected because the first generation was born from fresh material, enhanced in all  $\alpha$ -elements, including O. Instead the second generation was born from O-depleted material, which however had other  $\alpha$ -elements untouched. For Ruprecht 106 we found that the O content is only slightly lower than other  $\alpha$ -elements (0.07 dex), so we can say that the observed stars correspond to the first generation. With this information we can answer the following question: what is the probability that we have missed a second generation if present? Carretta et al. (2009) found that  $\sim 30$ -40% of stars now remaining in a GC belong to the first generation. We observed 9 stars and all belong to it. So the probability that we have missed the second population is:

$$P \sim 0.35^9 = 0.00008 = 0.008\%$$

This probability is low enough to confidently state that we did not miss any cluster sub-population. This would be true (however not in as clear a way) also if our stars had belonged to the second generation, for which we would obtain  $P=2\%$ . However, we recognize that our sample is still small, especially compared to the samples generally used to define the Na-O anticorrelation often with  $>100$  stars. Spectra of additional stars in Ruprecht 106 would be most welcome.

Another relevant piece of evidence comes from the HB. It has a dispersion in color of  $\sim 0.2$  mag (see Fig. 1). According to Caloi & D'Antona (2011) a dispersion of 0.3 mag or lower is an indication that no multiple populations are present in a cluster. So this fact further reinforces our main result.

The last possibility could be that Rup 106 represents one of those first generation-mainly clusters, where a second generation is present but not dominant (Caloi & D'Antona 2011). However in this case we should still see a HB extended to the blue because second generation HB stars populate a hotter and bluer HB part than first generation stars as discussed in the introduction. In Rup 106 this would correspond to HB stars with  $(V-I)<0.5$  (see Fig. 1), where no stars at all are present. On the other hand the chances that Rup 106 is such an object are decreased by the fact that first generation-mainly clusters are assumed to not have filled their tidal radius and thus did not lose

many first generation stars. However, odds with this, Rup 106 is known to be a tidally-filling cluster (Baumgardt et al. 2011). In conclusion, the evidence strongly points to Rup 106 as a first generation only cluster.

Considering the above factors, we conclude that it is very likely that Ruprecht 106 is the first confirmed example of a single population, globular cluster.

What about other possible candidates? One is Palomar 3. Caloi & D’Antona (2011) suggested it as a single population cluster based on its HB, that has a color spread of 0.25 mag (see their Fig. 2). For Ruprecht 106 instead we found a value  $\leq 0.20$  mag (see Fig. 1). On the spectroscopic side, Kock et al. (2009) found that the observed Na spread in Palomar 3 slightly exceeds that expected from theoretical errors and is not accompanied by a spread in O. This is not surprising because Palomar 3 stars are located in a region of the Na-O anticorrelation where little or no O variation is expected. In our opinion, these results together suggest that Palomar 3 has a small but real spread in light elements, and it is therefore probably not an example of a single population GC. In addition only 4 stars have been observed at high resolution. On the other hand, NGC 1783 and Terzan 7 have a dispersion in Na of 0.10 and 0.12 dex respectively, larger than Ruprecht 106, but that could be due to larger internal errors. So they could be single population GCs. In any case for these three clusters further investigation is required to reveal their nature. Obviously, it is of interest to observe other possible candidate single-population GCs.

We finally note that these candidates are extragalactic or, in the case of Palomar 3, probably have an extragalactic origin (Caloi & D’Antona 2011). This is true also for Ruprecht 106 (see next section). A possible reason could be that all low mass single population Galactic GC were destroyed due to the tidal interaction with the Milky Way, or simply they did not form at all. However, most low mass GCs have not been adequately investigated yet.

## 6. Additional photometric evidence

It is now well known that the U filter is able to disentangle multiple populations along the RGB of Globular Clusters (Marino et al. 2008;

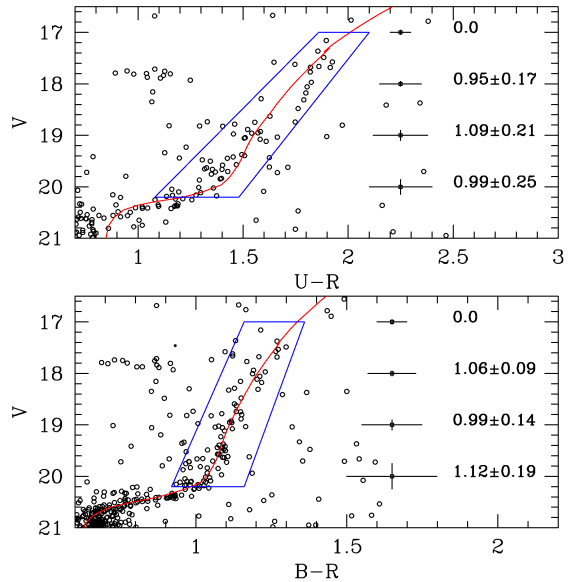


Fig. 5.— Upper panel: V vs. U-R CMD of the cluster zoomed on the RGB. Lower panel: V vs. B-R CMD of the cluster zoomed on the RGB.

Sbordone et al. 2011) due to its sensitivity to chemical inhomogeneities. For this purpose we extracted photometric material for Ruprecht 106 from the ESO public archive<sup>2</sup>. It consists of a series of images in UBVRI taken with the Superb Seeing Imager (SUSI2) at La Silla Observatory on the night of July 21, 2002. The detector has a scale of 0.08 arcsec/pixel, allowing to cover  $5.5 \times 5.4$  arcmin on the sky.

This data-set has the widest optical wavelength coverage for Ruprecht 106 available, and it is ideal to study the detailed shape of the Red Giant Branch. The night was photometric according to the weather report from ESO La Silla, with an average seeing of 0.8 arcsec in the V passbands. Exposures range from 30 to 900 in U, B, V, and R. The cluster was also observed in I, but the images show significant fringing, which made it impossible to extract good photometry. Only the north-east portion of the cluster was surveyed. After pre-reduction (bias and flat-field corrections) images have been reduced using the DAOPHOT/ALLSTAR routines. SUSI2 has two

<sup>2</sup>[http://archive.eso.org/eso/\\_archive\\_.main.html](http://archive.eso.org/eso/_archive_.main.html)

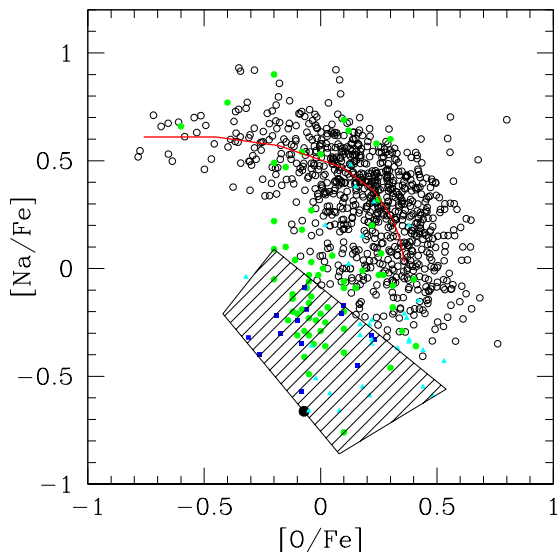


Fig. 6.— Na-O anticorrelation. Filled cyan triangles: Draco, Sextans, and Ursa Minor dwarf galaxies. Filled blue squares: Sagittarius dwarf galaxy. Filled green circles: LMC. Open black circles: GCs from Carretta et al. (2009). Filled black circle: Ruprecht 106. See text for more details.

detectors, which have been separated and reduced individually. The two extracted catalogs have then been merged. To tie the instrumental photometry to the standard system we used the average zero-points and color terms reported in the website of the instrument.<sup>3</sup>

In Fig. 5 we present a zoom on the RGB region in 2 different color combinations: V vs. U-R in the upper panel, and V vs. B-R in the lower, to maximize the color range of the stars. The V vs. B-R combination was included as a reference only, because colors other than U are not as sensitive to chemical inhomogeneities. We use the metallicity derived in this paper to fit the star distribution with theoretical isochrones (red lines) from the Padova database (Marigo et al. 2008). We find that the best-fitting parameters are an age of 12 Gyrs, a reddening  $E(B-V) = 0.19$ , and an apparent distance modulus  $(m-M)_V = 17.20$  mag. Both reddening and distance modulus are in good agreement with the literature value.

Color-coded in blue is the region where bona-fine RGB stars are located. Lacking any quantitative membership, these have been selected as the RGB stars lying within the cluster core region (core radius=1.0 arcmin, Harris 1996). Photometric errors, in magnitude and color, are also indicated with error-bars color-coded in black. To investigate a possible intrinsic photometric spread in the RGB, we compared its observed color scatter with the natural width expected from considering the photometric errors only. These are calculated as

$$\begin{aligned}\sigma_{B-R} &= 2 \times \sqrt{(\sigma_B^2 + \sigma_R^2)} \\ \sigma_{U-R} &= 2 \times \sqrt{(\sigma_U^2 + \sigma_R^2)}\end{aligned}$$

depending on the CMD. As for the observed color scatter at a given V, we simply consider the difference in color  $\Delta(B-R)$ , and  $\Delta(U-R)$  between the two most separated stars in the RGB at about the same V. This is because the RGB is not very rich, and therefore any other statistical calculation would be not robust. The results for 4 different V magnitudes are reported directly in the figure as  $\sigma/\Delta$  with their errors. Apart from the value at  $V = 17$ , where no RGB stars are located, the ratios are compatible with 1 within the errors, indicating that the RGB is not wider than the amount expected from photometric errors only. We therefore conclude that this photometric dataset supports the spectroscopic result that no significant spread exists among Ruprecht 106 RGB stars.

We can further compare our (U-R) vs. V CMD with that for M4 (Marino et al. 2008, (U-B) vs U, Fig. 11). M4 has a very broad RGB with a spread of  $\sim 0.2$  mag. in color. At odds with this, the Rup 106 RGB spread is only 0.1 mag. Because M4 has one of the lowest Na-O spreads among GCs (Carretta et al. 2009), we conclude that this photometry further supports our spectroscopic result.

## 7. Comparison with Galactic and extragalactic environments

The position of Ruprecht 106 stars in Fig. 4 is extraordinary. They do not fit any Na-O trend defined by Galactic GC. This is an indication that Ruprecht 106 has an extragalactic origin. In order to investigate this point more deeply, we compare our results with Galactic

<sup>3</sup><http://www.eso.org/sci/facilities/lasilla/>



and extragalactic environments. For this purpose, we plotted in Fig. 6 data for Galactic GCs (Carretta et al. 2009, open black circles) to trace the Na-O trend for the Galactic Halo. In addition we added data for the LMC field and cluster stars (Johnson et al. 2006; Pompeia et al. 2008; Mucciarelli et al. 2008, 2009, green filled circles), Sagittarius dwarf galaxy field and cluster stars (Sbordone et al. 2007, filled blue squares), the Draco, Sextans, and Ursa Minor dwarf galaxy field stars (Shetrone et al. 2001, filled cyan triangles). The continuous red line indicates the mean trend for a Galactic GCs. The main result is that, while the area occupied by the Galactic stars is common also to the extragalactic objects, there is a region occupied only by extragalactic stars, indicated by the shaded region, that are more Na-poor with respect to the Galactic Halo. Ruprecht 106 (the filled black circle) lies at the opposite extreme of this area, and because of this it can be considered with high confidence an extragalactic object.

Additional support for an extragalactic origin comes from Fig. 7. Here we plot the  $[\alpha/\text{Fe}]$  vs.  $[\text{Fe}/\text{H}]$  relation for extragalactic stars defined as in Fig. 6 and galactic field stars (red crosses) from the following sources: Fulbright (2000); Cayrel et al. (2004); Reddy et al. (2003); Barklem et al. (2005); Reddy et al. (2006). In this plot we added also LMC stars from Monaco et al. (2005).  $[\alpha/\text{Fe}]$  was defined as the mean abundance of Mg, Si, Ca, and Ti except for Pompeia et al. (2008); Barklem et al. (2005); Monaco et al. (2005) for which we used Mg, Ca, and Ti. For Mucciarelli et al. (2009) we were forced to use the only  $\alpha$ -element available (besides O), i.e. Mg. In any case, stars from Mucciarelli et al. (2009) follow the general trend of the LMC. First of all, in Fig. 7 we identified a double trend of  $[\alpha/\text{Fe}]$  vs.  $[\text{Fe}/\text{H}]$  for the Galaxy, where stars define a first continuous path from  $[\text{Fe}/\text{H}] \sim -3.5$  dex up to  $[\text{Fe}/\text{H}] \sim -0.2$  dex, indicated by the upper black dashed line. The second continuous path goes from  $[\text{Fe}/\text{H}] \sim -1.2$  up to  $[\text{Fe}/\text{H}] \sim +0.2$  and is indicated by the lower black dashed line. Between the two trends there is an almost empty region indicated by the blue shaded area. This result is not new and was recently noticed by Adibekyan et al. (2011). These authors found two distinct  $[\alpha/\text{Fe}]$  vs.  $[\text{Fe}/\text{H}]$  trends among Galactic stars, with an almost empty region between them (see their Fig.

1), exactly as in our case. Apart from that, we can see that extragalactic stars have the same mean  $\alpha$ -enhancement as the Milky Way up to  $[\text{Fe}/\text{H}] \sim -1.5$ . More metal rich extragalactic stars instead tend to have a much lower  $\alpha$  content than Galactic stars of the same metallicity. The black shaded area indicates the region populated only by extragalactic objects. Again Ruprecht 106 (the filled black circle) lies in this area well removed from any Galactic star.

Finally in Fig. 8 we compare the Ni and Cu content of Rup 106 with Galactic and extragalactic stars. Literature sources are those discussed above. Solar-scaled abundances are shown as continuous black lines for reference. As far as Ni is concerned, Galactic stars follow a solar-scaled trend with a large spread for  $[\text{Fe}/\text{H}] < -2$ . On the other hand, extragalactic objects are solar scaled below  $[\text{Fe}/\text{H}] = -1.5$ . Then they start to deviate, reaching  $[\text{Ni}/\text{Fe}] \sim -0.5$  for solar metallicity. Rup 106 is located at the metallicity where the deviation starts, but below the Galactic trend and fully compatible with extragalactic targets.

As for Cu, Galactic stars follow a solar scaled trend down to  $[\text{Fe}/\text{H}] \sim -0.9$ . Below that metallicity they drop to  $[\text{Cu}/\text{Fe}] \sim -0.4$ . Extragalactic targets are more Cu poor on average with  $\langle [\text{Cu}/\text{Fe}] \rangle \sim -0.6$  regardless of the iron content. Although the number of Galactic stars at the metallicity of Ruprecht 106 is very small, our cluster is again located below the Galactic trend and fully compatible with extragalactic targets, once again pointing to an extragalactic origin.

It is of course very difficult to say where Ruprecht 106 comes from. It was suggested initially to be part of the Sagittarius dwarf galaxy (Bellazzini et al. 2003), but Law & Majewski (2010) discarded this hypothesis because it does not belong to any possible stream of this system, so we regard its exact origin as an open question, but an extragalactic formation is strongly favoured by our data.

## 8. Summary and conclusions

In this paper we present detailed chemical abundances of red giants in the globular cluster Ruprecht 106. We studied 29 elements from C to Pb, including light,  $\alpha$ , iron-peak, and neutron-capture. Our main aim was to investigate if

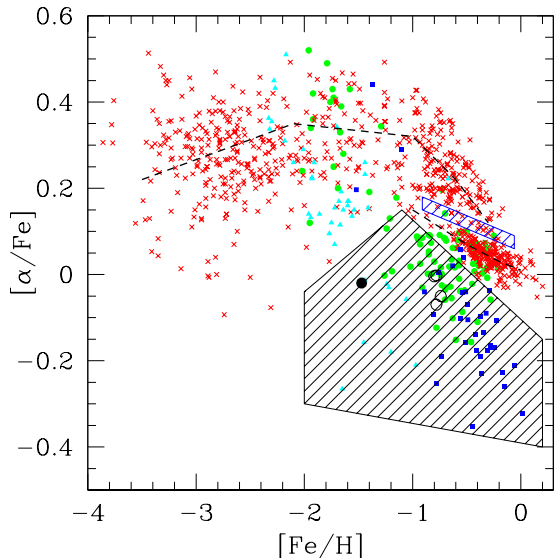


Fig. 7.—  $[\alpha/\text{Fe}]$  vs.  $[\text{Fe}/\text{H}]$ . Filled cyan triangles: Draco, Sextans, and Ursa Minor dwarf galaxies. Filled blue squares: Sagittarius dwarf galaxy. Filled green circles: LMC. Red crosses: Milky Way. Filled black circle: Ruprecht 106. See text for more details.

Ruprecht 106 is a single population GC. All GCs studied up to now show some spread in their chemical abundances. There are a few examples where no spread was found, but those results are doubtful due to the small sample of stars observed and to the lack of an accurate error analysis. We analyzed 9 member stars and performed an accurate error abundance analysis. We found that the observed spread in all elements, in particular Na and O, is totally within the measurement errors. We calculated also a negligible probability of having missed stars with an intrinsic difference in their chemical content with respect to our targets given the nominal ratio of first to second generation stars. This is also confirmed by the small color spread of the HB. No intrinsic abundance spread is present in this GC in any element. Although our sample is still relatively small and more observations would be of great interest, our evidence strongly suggests that Ruprecht 106 is the first genuine old, massive GC with only a single population.

In addition, we could establish the following:

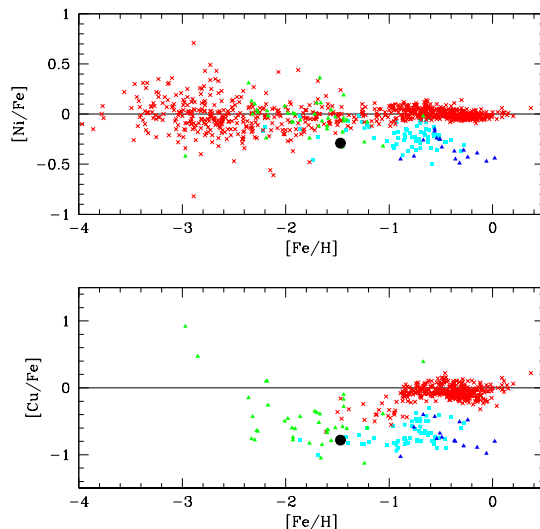


Fig. 8.—  $[\text{Ni}/\text{Fe}]$  vs.  $[\text{Fe}/\text{H}]$  and  $[\text{Cu}/\text{Fe}]$  vs.  $[\text{Fe}/\text{H}]$ . Filled cyan triangles: Draco, Sextans, and Ursa Minor dwarf galaxies. Filled blue squares: Sagittarius dwarf galaxy. Filled green circles: LMC. Red crosses: Milky Way. Filled black circle: Ruprecht 106. See text for more details.

- Ruprecht 106 has  $[\text{Fe}/\text{H}] \sim -1.5$  and  $[\alpha/\text{Fe}] \sim 0.0$ . This solves the disagreement in the literature between metallicity measurements based on photometry or low resolution spectroscopy and those based on high resolution spectroscopy.
- Its neutron-capture element abundances point toward a contamination of the gas the cluster was formed from by both the s and r processes. The contamination fraction is  $\sim 30\%$  and  $70\%$  respectively.
- NGC 1783, Terzan 7, and Palomar 3 are candidate single population GCs. Available data are uncertain and new more accurate studies are required to confirm their nature.
- Na/O,  $\alpha$ , and iron-peak abundances clearly point toward an extragalactic origin of the cluster. No progenitor galaxy or stream have been clearly identified yet.

Ruprecht 106 has a present day mass of  $M = 10^{4.83} M_{\odot}$ . This is not its initial mass because it lost a fraction of its stars due to internal

precesses and to interaction with the Milky Way. A determination of the initial mass would require the knowledge of its orbit and a detailed dynamical simulation. This is beyond the scope of this paper. In any case we can fix  $M=10^{4.83} M_{\odot}$  as a lower limit for the initial mass threshold below which no ejecta are retained by the gravitational potential of a cluster and no second generation of stars is formed. Note that NGC 6838, one of the Carretta et al. (2009) sample clusters, has a present day mass of  $M=10^{4.30} M_{\odot}$ , much less than that of Ruprecht 106, but shows a real Na-O spread. We hypothesize that NGC 6838 was originally more massive than Ruprecht 106, but subsequently lost more mass.

S.V. and D.G. gratefully acknowledge support from the Chilean Centro de Excelencia en Astrofísica y Tecnologías Afines (CATA) grant PFB-06/2007. The authors gratefully acknowledge also Ata Sarajedini who kindly provided the ACS@HST photometry. S.V. gratefully acknowledges the support provided by FONDECYT N. 1130721

## REFERENCES

- Adibekyan, V.Z., Santos, N.C., Sousa, S.G., & Israelian, G. 2011, arXiv1111.4936
- Alonso, A., Arribas, S. & Martínez-Roger, C. 1999, A&AS, 140, 261
- Barklem, P.S., Christlieb, N., Beers, T.C., Hill, V., Bessell, M.S., Holmberg, J., Marsteller, B., Rossi, S., Zickgraf, F.J., & Reimers, D. 2005, A&A, 439, 129
- Baumgardt, H., Lockmann, U. & Kroupa, P. 2011, ASPC, 439, 96
- Bellazzini, M., Ferraro, F.R., & Iata, R. 2003, AJ, 125, 188
- Brown, J.A., Wallerstein, G., & Zucker, D. 1997, AJ, 114, 180
- Buonanno, R., Buscema, G., Fusi Pecci, F., Richer, H.B., & Fahlman, G.G. 1990, AJ, 100, 1811
- Busso, M., Gallino, R., Lambert, D.L., Travaglio, C., & Smith, V.V. 2001, ApJ, 557, 802
- Cayrel, R., Depagne, E., Spite, M., Hill, V., Spite, F., Francois, P., Plez, B., Beers, T., Primas, F., Andersen, J. 2004, A&A, 416, 1117
- Caloi, V., & D’Antona, F. 2011, MNRAS, 417, 228
- Carraro, G., Villanova, S., Demarque, P., McSwain, M.V., Piotto, G., & Bedin, L.R. 2006, ApJ, 643, 1151
- Carretta, E., Bragaglia, A., Gratton, R.G., Leone, F., Recio-Blanco, A., & Lucatello, S. 2006, A&A, 450, 523
- Carretta, E., Bragaglia, A., Gratton, R.G., Lucatello, S., & Momany, Y. 2007, A&A, 464, 927
- Carretta, E., Bragaglia, A., Gratton, R.G., Lucatello, S., Catanzaro, G., Leone, F., Bellazzini, M., Claudi, R., D’Orazi, V., & Momany, Y. 2009, A&A, 505, 117
- Carretta, E., Bragaglia, A., Gratton, R.G., Lucatello, S., Bellazzini, M., Catanzaro, G., Leone, F., Momany, Y., Piotto, G. & D’Orazi, V. 2010, A&A, 520, 95
- D’Antona, F., Caloi, V., Montalbán, J., Ventura, P., & Gratton, R. 2002, A&A, 395, 69
- D’Antona, F., & Caloi, V. 2008, MNRAS, 390, 693
- de Silva, G.M., Gibson, B.K., Lattanzio, J., & Asplund, M. 2009, A&A, 500, 25
- Decressin, T., Meynet, G., Charbonnel, C., Prantzos, N., & Ekstrom, S. 2007, A&A, 464, 1029
- D’Ercole, A., Vesperini, E., D’Antona, F., McMillan, S.L.W., & Recchi, S. 2008, MNRAS, 391, 825
- Da Costa, G.S., Armandroff, T.E., & Norris, J.E. 1992, AJ, 104, 154
- Dotter, A., Sarajedini, A., & Anderson, J. 2011, ApJ, 738, 74
- Francois, P., Danziger, J., Buonanno, R., & Perrin, M. N. 1997, A&A, 327, 121
- Fulbright, J.P. 2000, AJ, 120, 1841
- Gratton, R., Sneden, C., & Carretta, E. 2004, ARA&A, 42, 385

- Gratton, R. G., Lucatello, S., Carretta, E., et al. 2011, *A&A*, 534, A123
- Gratton, R. G., Lucatello, S., Carretta, E., et al. 2012, *A&A*, 539, A19
- Gratton, R. G., Lucatello, S., Sollima, A., et al. 2013, *A&A*, 549, A41
- Grevesse, N. & Sauval, A.J. 1998, *SSRv*, 85, 161
- Geisler, D., Wallerstein, G., Smith, V.V., & Casetti-Dinescu, D.I. 2007, *PASP*, 119, 939
- Geisler, D., Villanova, S., Carraro, G., Pilachowski, C., Cummings, J., Johnson, C. I., & Bresolin, F. 2012, *ApJ*, 756, 40
- Harris, W.E. 1996, *AJ*, 112, 1487
- Johnson, J.A., Ivans, I.I., & Stetson, P.B. 2006, *ApJ*, 640, 801
- Johnson, C.I. & Pilachowski, C.A. 2010, *ApJ*, 722, 1373
- Karakas, A. & Lattanzio, J.C. 2007, *PASA*, 24, 103
- Koch, A., Coté, P., & McWilliam, A. 2009, *A&A*, 506, 729
- Kraft, R. P. 1994, *PASP*, 106, 553
- Kurucz, R.L. *SAO*, 309
- Law, D.R., & Majewski, S.R. 2010, *ApJ*, 718, 1128
- Maccarone, T. J., & Zurek, D. R. 2012, *MNRAS*, 423, 2
- McWilliam, A. 1997, *ARA&A*, 35, 503
- Mandushev, G., Staneva, A., & Spasova, N. 1991, *A&A*, 252, 94
- Marino, A.F., Villanova, S., Piotto, G., Milone, A.P., Momany, Y., Bedin, L.R. & Medling, A.M. 2008, *A&A*, 490, 625
- Marino, A.F., Milone, A.P., Piotto, G., Villanova, S., Bedin, L.R., Bellini, A. & Renzini, A. 2009, *A&A*, 505, 1099
- Marino, A.F., Villanova, S., Milone, A.P., Piotto, G., Lind, K., Geisler, D., & Stetson, P.B. 2011, *ApJ*, 730L, 16
- Mashonkina, L.I., Shimanskii, V. V., & Sakhbullin, N.A. 2000, *ARep*, 44, 790
- de Mink, S. E., Pols, O. R., Langer, N., & Izzard, R. G. 2009, *A&A*, 507, L1
- Monaco, L., Bellazzini, M., Bonifacio, P., Ferraro, F.R., Marconi, G., Pancino, E., Sbordone, L., & Zaggia, S. 2005, *A&A*, 441, 141
- Mucciarelli, A., Carretta, E., Origlia, L., & Ferraro, F.R. 2008, *AJ*, 136, 375
- Mucciarelli, A., Origlia, L., Ferraro, F.R., & Pancino, E. 2009, *ApJ*, 695, 134
- Reddy, B.E., Tomkin, J., Lambert, D.L., & Allende Prieto, C. 2003, *MNRAS*, 340, 304
- Reddy, B.E., LambeSp05rt, D.L., & Allende Prieto, C. 2006, *MNRAS*, 367, 1329
- Roederer, I.U., Kratz, K.L., Frebel, A., Christlieb, N., Pfeiffer, B., Cowan, J.J., & Sneden, C. 2009, *ApJ*, 698, 1963
- Pignatari, M., Gallino, R., Meynet, G., Hirschi, R., Herwig, F., & Wiescher, M. 2008, *ApJ*, 687, 95
- Piotto, G. 2009, *IAUS*, 258, 233
- Piotto, G., Milone, A.P., Anderson, J., Bedin, L.R., Bellini, A., Cassisi, S., Marino, A.F., Aparicio, A., Nascimbeni, V. 2012, *ApJ*, 760, 39
- Pompéia, L., Hill, V., Spite, M., Cole, A., Primas, F., Romaniello, M., Pasquini, L., Cioni, M.R., & Smecker Hane, T. 2008, *A&A*, 480, 379
- Sarajedini, A., & Layden, A. 1997, *AJ*, 113, 264
- Sbordone, L., Bonifacio, P., Buonanno, R., Marconi, G., Monaco, L., & Zaggia, S. 2007, *A&A*, 465, 815
- Sbordone, L., Salaris, M., Weiss, A., & Cassisi, S. 2011, *A&A*, 534, 9
- Shetrone, M.D., Coté, P., & Sargent, W.L.W. 2001, *ApJ*, 548, 592

- Snedden, C. 1973, ApJ, 184, 839
- Snedden, C., Cowan, J.J., & Gallino, R. 2008, ARA&A, 46, 241
- Valcarce, A. A. R., & Catelan, M. 2011, A&A, 533, 120
- Ventura, P., D'Antona, F., Mazzitelli, I., & Gratton, R. 2001, ApJ, 550, L65
- Villanova, S., Geisler, D., & Piotto, G. 2010, ApJ, 722, 18
- Villanova, S., & Geisler, D. 2011, A&A, 535, 31